ALUMINUM PHOSPHATE–SULFATE MINERALS ASSOCIATED WITH PROTEROZOIC UNCONFORMITY-TYPE URANIUM DEPOSITS IN THE EAST ALLIGATOR RIVER URANIUM FIELD, NORTHERN TERRITORIES, AUSTRALIA

Stéphane GABOREAU[§], Daniel BEAUFORT, Philippe VIEILLARD and Patricia PATRIER

HydrASA, Université de Poitiers, CNRS–UMR 6532, 40, avenue du Recteur Pineau, F–86022 Poitiers Cedex, France

Patrice BRUNETON

COGEMA–BUM–DEX, 2, rue Paul Dautier, BP 4 , F–78141 Vélizy Cedex, France

ABSTRACT

Aluminum phosphate–sulfate (APS) minerals occur as disseminated crystals in a wide range of geological environments near the Earth's surface, including weathering, sedimentary, diagenetic, hydrothermal, metamorphic and also postmagmatic systems. Their general formula is $AB_3(XO_4)_2(OH)_6$, in which *A*, *B* and *X* represent three different crystallographic sites. These minerals are known to incorporate a great number of chemical elements in their lattice and to form complex solid-solution series controlled by the physicochemical conditions of their formation (Eh, pH, activities of constituent cations, P and T). These minerals are particularly widespread and spatially related to hydrothermal clay-mineral parageneses in the East Alligator River Uranium Field (EARUF) environment associated with uranium orebodies in the Proterozoic Kombolgie basin of the Northern Territories, Australia. This field contains several high-grade unconformity-related uranium deposits, including Jabiluka and Ranger. Both petrography and chemical data are used to discuss the significance of APS minerals in the alteration processes from the EARUF. The wide range of chemical compositions recorded in APS is essentially due to coupled substitutions of Sr for the LREE and of S for P at the *A* and *X* sites, respectively. The major variations of the APS solid-solution series mainly consist of the relative proportions of svanbergite, goyazite and florencite end-members. The APS minerals result from the interaction of oxidizing and relatively acidic fluids with aluminous host-rocks enriched in monazite. The spatial distribution of these minerals and their compositional variation around the uranium orebodies allow us to consider them as good tracers of redox and pH paleo-conditions responsible for the development of fronts during the alteration processes, and hence as potential tools for mineral exploration.

Keywords: aluminum sulfate–phosphate minerals, florencite, goyazite, svanbergite, unconformity-type uranium deposits, clay minerals, paleo-conditions of redox and pH, East Alligator River Uranium Field, Australia.

SOMMAIRE

Les sulfates-phosphates d'aluminium (APS) sont des minéraux ubiquistes disséminés dans un grand nombre d'environnements géologiques: sédimentaire, diagénétique hydrothermal, métamorphique, magmatique. Leur formule générale est $AB_3(XO_4)_2(OH)_6$, dans laquelle *A*, *B* et *X* correspondent à trois sites cristallographiques. Ces minéraux sont connus pour intégrer un grand nombre d'éléments chimiques dans leur structure sous la forme de nombreuses solutions solides dont la nature est contrôlée par les conditions de formation (Eh, pH, activités des éléments chimiques, P et T). Ces minéraux sont particulièrement répandus dans le district de l'East Alligator River Uranium Field (Territoires du Nord, Australie), où ils accompagnent les altérations argileuses autour des gisements d'uranium de type discordance, d'âge protérozoïque. Ce district contient plusieurs gisements d'uranium, de rang économique, tel que Jabiluka et Ranger. Les observations pétrographiques et les analyses chimiques effectuées lors de cette étude ont été utilisées pour discuter de l'intérêt des APS au niveau des altérations observées dans le district de l'East Alligator River Uranium Field. La diversité des compositions chimiques enregistrée par les APS dans ce district est essentiellement due aux substitutions de Sr aux terres rares légères et de S à P, respectivement dans les sites *A* et *X*. Les variations majeures observées dans ces solutions solides concernent la proportion relative des pôles purs svanbergite, goyazite et florencite. La formation des APS résulte de l'interaction entre un fluide relativement acide et oxydant et des roches riches en monazite et minéraux alumineux. La distribution spatiale de ces minéraux et leur variation cristallochimique par rapport aux gisements d'uranium nous permet de considérer ces minéraux comme de bons marqueurs des paléo-conditions redox et pH responsables du développement des fronts d'altération et, par conséquent, comme un guide potentiel pour l'exploration minière de ces gisements.

Mots-clés: sulfates-phosphates d'aluminium, florencite, goyazite, svanbergite, gisement d'uranium de type discordance, minéraux argileux, paléo-conditions redox et pH, East Alligator River Uranium Field, Australie.

[§] *E-mail address*: stephane.gaboreau@hydrasa.univ-poitiers.fr

INTRODUCTION

Aluminum phosphate–sulfate (APS) minerals occur as disseminated grains in a wide range of geological environments near the Earth's surface, including weathering, sedimentary, diagenetic, hydrothermal, metamorphic and postmagmatic systems (Dill 2001). APS minerals belong to the alunite supergroup (Scott 1987, Jambor 1999) and crystallize most commonly as authigenic rhombohedral crystals. Their general formula is ideally $AB_3(XO_4)_2(OH)_6$, in which A, B and X represent three different crystallographic sites: 12-fold coordinated A sites, occupied by monovalent (H_3O, K, Na, Rb, NH_4, Ag, Tl, *etc*.), divalent (Ca, Sr, Ba and Pb, *etc*.), trivalent (Bi and rare-earth elements, REE) and, more rarely, tetravalent (Th) cations; 6-fold coordinated B sites, occupied by Al^{3+}, Fe^{3+} and, more rarely, Ga^{3+} or V^{3+}; 4-fold coordinated X sites, occupied by S^{6+}, P^{5+}, As^{5+}, and, more rarely, by Cr^{6+}, Sb^{5+} and minor Si^{4+}.

APS minerals have been neglected by geologists and geochemists because of the minute size of the crystals ($<0.1–10$ μm) and their low concentration (generally less than 0.05 wt%), which hindered their identification by conventional microscopic techniques. At the same time, their marked insolubility at low temperature also rendered them inert to sequential extraction in solvents. However, several studies in the last ten years have pointed out the interest of APS minerals for Earth scientists who deal with paleoconditions in natural systems and with environmental problems: (1) APS minerals are highly sensitive to their physicochemical conditions of formation through a wide range of compositional variations, owing to complex solid-solutions among more than 20 end-members (Stoffregen 1993, Stoffregen *et al.* 1994, Jambor 1999, Mordberg *et al.* 2000). After crystallization, these minerals become very resistant to weathering and dissolution, and are ubiquitous minerals in near-surface environments. (2) APS minerals represent an important sink for reactive P and large amounts of trace elements incorporated in their structure, which has been neglected in the global budget of chemical elements at the Earth's surface (Rasmussen 1996).

APS minerals are particularly abundant in the clay assemblages associated with some uranium fields in the middle Proterozoic basins. These fields contain several high-grade unconformity-type uranium deposits, and several unexplored important prospects in Canada and Australia (Miller 1983, Wilson 1984, Quirt *et al.* 1991, Fayek & Kyser 1997, Lorilleux 2001, Beaufort *et al.* 2005). No systematic investigations have been performed on the APS minerals in these deposits, and no data are available on their compositional variations in relation to the uranium deposits, though it is well known that their emplacement was controlled by physicochemical conditions (Eh, pH, activities of constituent metals, P and T), to which APS are particularly sensitive (Dill 2001, Kolitsch & Pring 2001).

The aim of this study are to clarify the nature and the origin of the APS minerals on both sides of the middle Proterozoic unconformity between the overlying Kombolgie sandstones and the underlying metamorphic basement rocks that host the uranium orebodies of the East Alligator River Uranium Field (EARUF). Spatial variations of both crystal chemistry and phase relationships with clay minerals, on a regional scale, have been investigated in order to improve our knowledge on the suitability of these minerals to indicate the paleoconditions at which the alteration processes relative to the uranium deposition operated.

REGIONAL GEOLOGICAL SETTING

The East Alligator River Uranium Field (EARUF) is located to the east of the Pine Creek Geosyncline, close to the Kakadu Group, which is a part of the North Australian Craton. The oldest rocks of the EARUF correspond to Archean granitic gneisses of the Nanambu Complex, which form the basement to the west (in the Jabiru area). The complex is overlain by a thick early Proterozoic metamorphic sequence, composed of arkosic metasedimentary units, in turn overlain by the Cahill Formation, which includes calcareous rocks, carbonaceous schists and amphibolites, and host the major uranium deposits (Ranger 1, Ranger 3, Jabiluka and Koongarra) known in the Jabiru area (Needham 1988). East of the East Alligator River, in western Arnhem Land, the Cahill Formation grades into metamorphically differentiated schists, gneisses and amphibolites of the Myra Falls Metamorphic Complex, which contains the Nabarlek deposit. These rocks partly surround the granitic and migmatitic Nimbuwah Complex.

This Paleo- to Mesoproterozoic basement is unconformably overlain by a thick (5–15 km) middle Proterozoic cover forming the large intracratonic McArthur Basin. This sequence of nearly flat-lying sedimentary rocks, interpreted to have formed in terrestrial and marine environments (Kyser *et al.* 2000), corresponds to the Kombolgie Subgroup, part of the Katherine River Group (Sweet *et al.* 1999). The Kombolgie Subgroup, which is about 1500 m thick, was deposited in a mainly braided stream environment punctuated by brief intervals of marine deposition (Ojakangas 1986). The Kombolgie Subgroup consists of at least three units of sandstones and conglomerates separated by volcanic units. More details on the stratigraphy, lithology, and structure of the Kombolgie sandstones may be found in Gustafson & Curtis (1983). The age of the Kombolgie Subgroup has been constrained between 1822 and 1720 Ma (Sweet *et al.* 1999).

The main characteristics of the EARUF unconformity-type uranium deposits were summarized by Wilde *et al.* (1989) and Maas (1989). There is a close spatial relationship between the mineralized zones and the middle Proterozoic unconformity. The genetic models proposed for these uranium deposits are based on

the interaction of hypersaline, oxidizing and acidic basinal fluids originating in the Kombolgie sandstones with the underlying metamorphic basement rocks, and in turn, a progressive reduction and neutralization of the hydrothermal solutions with time (Komninou & Sverjensky 1996). Most of the primary uranium mineralization (dominantly uraninite) is located within and adjacent to reverse fault-zones and their associated breccias, which are post-Kombolgie in age. Mineralization is invariably accompanied by an intense alteration in which clay minerals constitute most of the newly formed minerals (Gustafson & Curtis 1983, Wilde *et al.* 1989, Nutt 1989). Hydrothermal alteration occurred in halos surrounding the mineralized zones, up to several hundreds of meters from the ore (Gustafson & Curtis 1983, Wilde *et al.* 1989), and extended along the structural discontinuities that represent the permeable zones (faults, fractures, and breccias) on both sides of the middle Proterozoic unconformity (Beaufort *et al.* 2005). In both the basement rocks and the overlying sandstones, alteration resulted in illite and chlorite formation, with accompanying dissolution of quartz. Minute crystals of APS were observed in association with most of the clay minerals formed during the various stages of alteration that constitute the alteration halo associated with uranium mineralization in the EARUF area (Beaufort *et al.* 2005).

SAMPLING

Eleven representative core samples were selected from a set of 220 core samples from 25 diamond drill-holes covering seven distinctive areas (Fig. 1). These samples have previously been studied in detail for alteration petrology and crystal chemistry of clay minerals (Beaufort *et al.* 2005). These samples (Table 1) were chosen on the basis of the following criteria: (1) host-rock petrography, (2) lateral distance to the orebodies or to identified uranium anomalies, (3) vertical distance to the unconformity, and (4) lateral distance to faults or brecciated zones. The samples are from the vicinity of major uranium deposits (Jabiluka, Nabarlek and Ranger) or mineralized prospects (Caramal, South Horn, SML Boundary) and from exploration drill-holes in western Arnhem Land. This sampling included a drill hole (U65–3) considered representative of the regional background of the Kombolgie sandstones. This drill hole intersects the lowermost Kombolgie units overlying the unconformity far from any known uranium anomaly and presents only minor traces of alteration close to the unconformity (Patrier *et al.* 2003).

METHODS

Samples were examined in polished thin section using an Olympus BH2 polarizing microscope. Freshly fractured rock fragments and polished thin sections were studied with a JEOL JSM6400 scanning electron microscope (SEM) equipped with an energy-dispersion spectrometer (EDS) for chemical analysis. SEM observations for morphological investigations were made in secondary electron mode on gold-coated slabs and in back-scattered electron (BSE) mode for identification of APS on the basis of chemical contrasts in carbon-coated polished thin sections. The conditions of observation were as follows: current intensity, 0.6 nA, and accelerating voltage, 15 kV.

Electron-microprobe analyses were made with a CAMECA SX50 using wavelength-dispersion spectrometer (WDS). We sought Al, Sr, P, Ca, La, Ce, Nd, Pr, Fe, S, Th and U. The instrument was calibrated using the following synthetic and natural standards: $SrSiO_3$, apatite, monazite, pyrite, NdCu, glass doped in rare-earth elements, UO_2 and La_3ReO_8. Corrections were made with a ZAF program. The analytical conditions were as follows: current intensity 20 nA, accelerating voltage 15 kV, spot size 2–4 mm, counting time 30 to 40 s per element. The relative error on the elements sought is below 1.5%. The structural formulas of APS minerals were calculated on the basis of one atom of *A*, two (XO_4) groups, and three *B*-site atoms per formula unit (Scott 1987).
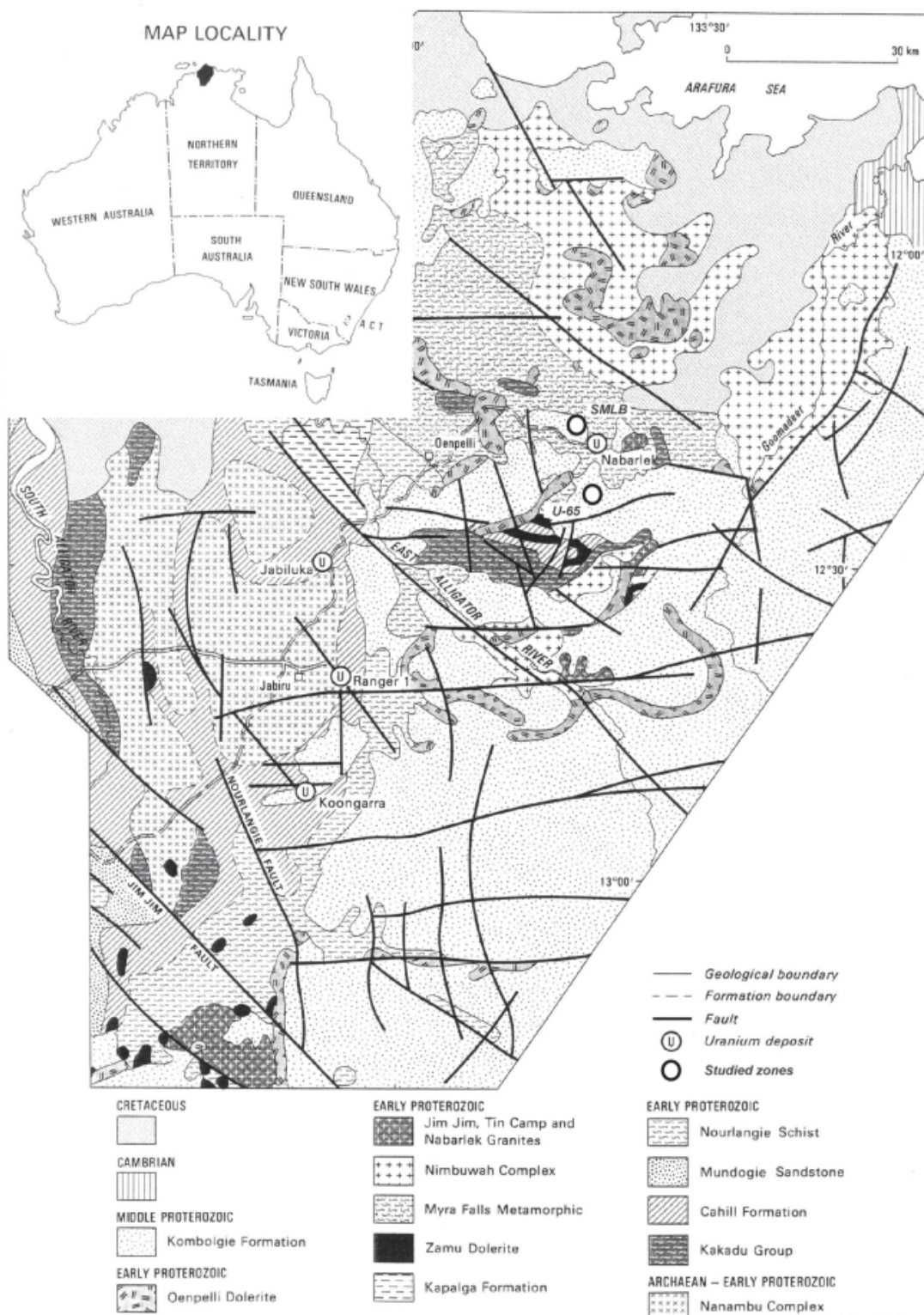
RESULTS

Petrographic relationships between APS and hydrothermal clay phases

Several APS-bearing clay-mineral assemblages have been distinguished as a function of the distance from the uranium orebodies or from the structural discontinuities that focused the hydrothermal solutions during mineralization events. At a regional scale, three main types of alteration zones can be distinguished on the basis of both the overall intensity of the alteration and the nature of the clay paragenesis: (1) *zones of proximal*

TABLE 1. PETROLOGICAL OBSERVATIONS OF THE VARIOUS SAMPLES ASSOCIATED WITH UNCONFORMITY-TYPE URANIUM DEPOSITS IN THE EAST ALLIGATOR RIVER URANIUM FIELD

Samples	Location	Non-APS minerals identified	Host rocks
1-3	Jabiluka, Ranger 3, Nabarlek deposits	Trioctahedral chlorite, monazite, pyrite	Altered metamorphic rocks, below the unconformity
4-6	SML Boundary Fault prospect	Illite, sudoite, ± trioctahedral chlorite, monazite, apatite, pyrite	Altered metamorphic rocks, close to the unconformity and discontinuities
7-8	SML Boundary Fault prospect	Illite, sudoite	Altered sandstone above and close to the unconformity
9	Regional background	Illite, hematite	Unaltered Kombolgie sandstone, above the unconformity

MAP LOCALITY

	Geological boundary
	Formation boundary
	Fault
Ⓤ	Uranium deposit
◯	Studied zones

CRETACEOUS		EARLY PROTEROZOIC		EARLY PROTEROZOIC	
			Jim Jim, Tin Camp and Nabarlek Granites		Nourlangie Schist
CAMBRIAN			Nimbuwah Complex		Mundogie Sandstone
			Myra Falls Metamorphic		Cahill Formation
MIDDLE PROTEROZOIC			Zamu Dolerite		Kakadu Group
	Kombolgie Formation		Kapalga Formation	ARCHAEAN – EARLY PROTEROZOIC	
EARLY PROTEROZOIC					Nanambu Complex
	Oenpelli Dolerite				

alteration, in which intense and zoned alteration-induced features occur as far as several hundred of meters around the economic uranium orebodies, located in the basement rocks below the unconformity, (2) *zones of intermediate alteration*, in which more or less intense and zoned alteration-induced features occur as far as several tens of meters around the unconformity and the regional faults, in areas where anomalous but subeconomic amounts of uranium have been detected, and (3) *zones of distal alteration*, in which weak alteration-induced features occur only close to the unconformity between the Kombolgie sandstone cover and the underlying metamorphic basement rocks, farther than 10 km from any known uranium deposit or prospect.

In both the proximal and the intermediate zones, the alteration halo is centered on the unconformity and the major faults that cross-cut the overlying sedimentary formations and the underlying basement rocks. The main difference between these two zones consists in the width of the alteration halo and the occurrence of massive chlorite near the uranium orebodies in the proximal areas. In both the proximal and the intermediate zones, alteration involves the intense dissolution of all the earlier silicates (including quartz) and the strong transformation of both the sedimentary and the metamorphic rocks above and below the unconformity to clay-mineral assemblages (Gustafson & Curtis 1983, Wilde *et al.* 1989). Minute crystals of APS were observed in the clay matrix by SEM because of their brightness in BSE mode, due to their high content in heavy elements such as Sr and LREE. Crystals of APS occur as very small euhedral rhombs (2–10 μm in average width, exceptionally up to 50 μm) located in the intergranular pore-space of the clay matrix, which constitutes most of the alteration products (Fig. 2a). Locally in the basement rocks, coarser-grained APS crystals display features of growth zoning characterized by alternation of thin concentric bright and light grey zones, less than 1 μm wide (Fig. 2b), reflecting chemical variations.

Globally, the mineralogical composition of the APS-bearing assemblages displays a zonal pattern as a function of the distance to the structures that focused the hydrothermal solutions and probably controlled the uranium deposition in these areas. The following assemblages have been identified: 1) illite + APS ± hematite, in the sandstones farther than several tens of meters above the unconformity (Fig. 2a), 2) illite + sudoite + APS ± hematite, on both sides close to the unconformity and close to the regional faults that reworked both sandstones and the basement rocks above and below the unconformity (Fig. 2c), 3) illite ± sudoite ± trioctahedral chlorite ± APS ± apatite, in the basement rocks at greater depth below the unconformity, and 4) massive trioctahedral chlorite ± APS ± apatite ± uraninite, close to the uranium orebodies (Fig. 2d).

In the distal zones, the alteration assemblage is composed of assemblage 1. APS minerals are disseminated in the clay matrix, whose illite crystals differ from diagenetic illite (in sandstones) or phengitic micas (in the metamorphic rocks) by their texture and their structure. Such illite consists of very fine-grained (less than 1 μm) capillary particles and $1M_{Trans}$ as the dominant polytype (Beaufort *et al.* 2005). Close to the unconformity, this illite matrix is superimposed upon the coarse-grained diagenetic illite of the altered sandstones, whereas it tends to replace the primary silicates in the underlying basement rocks.

Petrographic relationships between APS and other phosphate minerals

Several alteration-induced assemblages have been observed within the basement rocks from both the proximal and the intermediate zones of alteration. The APS ± secondary apatite are closely associated with the alteration of monazite. Residue of strongly etched crystals of monazite have been observed inside the APS crystals from the zones of massive chlorite formation that surround the ore deposits at Jabiluka and Ranger (Fig. 2d). Numerous indications of alteration and replacement of monazite by secondary phosphate minerals have been observed along regional faults, along metabasic rocks of the basement at more than one hundred meters below the unconformity. In these samples, ragged and frayed residues of coarse-grained monazite still persist in the illite + trioctahedral chlorite clay matrix, which replaces all the earlier silicate minerals (Fig. 2e). Grains of secondary subhedral to euhedral apatite are only observed close to the residue of monazite (Fig. 2f), whereas euhedral APS crystals are disseminated in the clay matrix slightly farther from the site of alteration of the monazite (Fig. 2e). Observations of the clay matrix surrounding the APS crystals at higher magnification reveal the presence of tiny residual grains of monazite and pyrite. The relationships between APS and apatite are complex. Detrital apatite was not observed in the altered sandstones, whereas coarse-grained, pore-sealing, diagenetic apatite was locally observed in sandstone samples containing APS disseminated in the illite matrix near the bottom of the sedimentary basin. These coarse grains of apatite show many features attributed to dissolution, but no evidence of a direct replacement by APS. At least two distinct generations of apatite were encountered in the basement rocks below the unconformity: partially dissolved, coarse-grained and globular crystals of primary apatite and fine-grained subhedral to euhedral crystals of apatite that surround

FIG. 1. Location of the study area on a geological map of the East Alligator River Uranium Field (EARUF), Northern Territory, Australia (modified from Needham 1988).
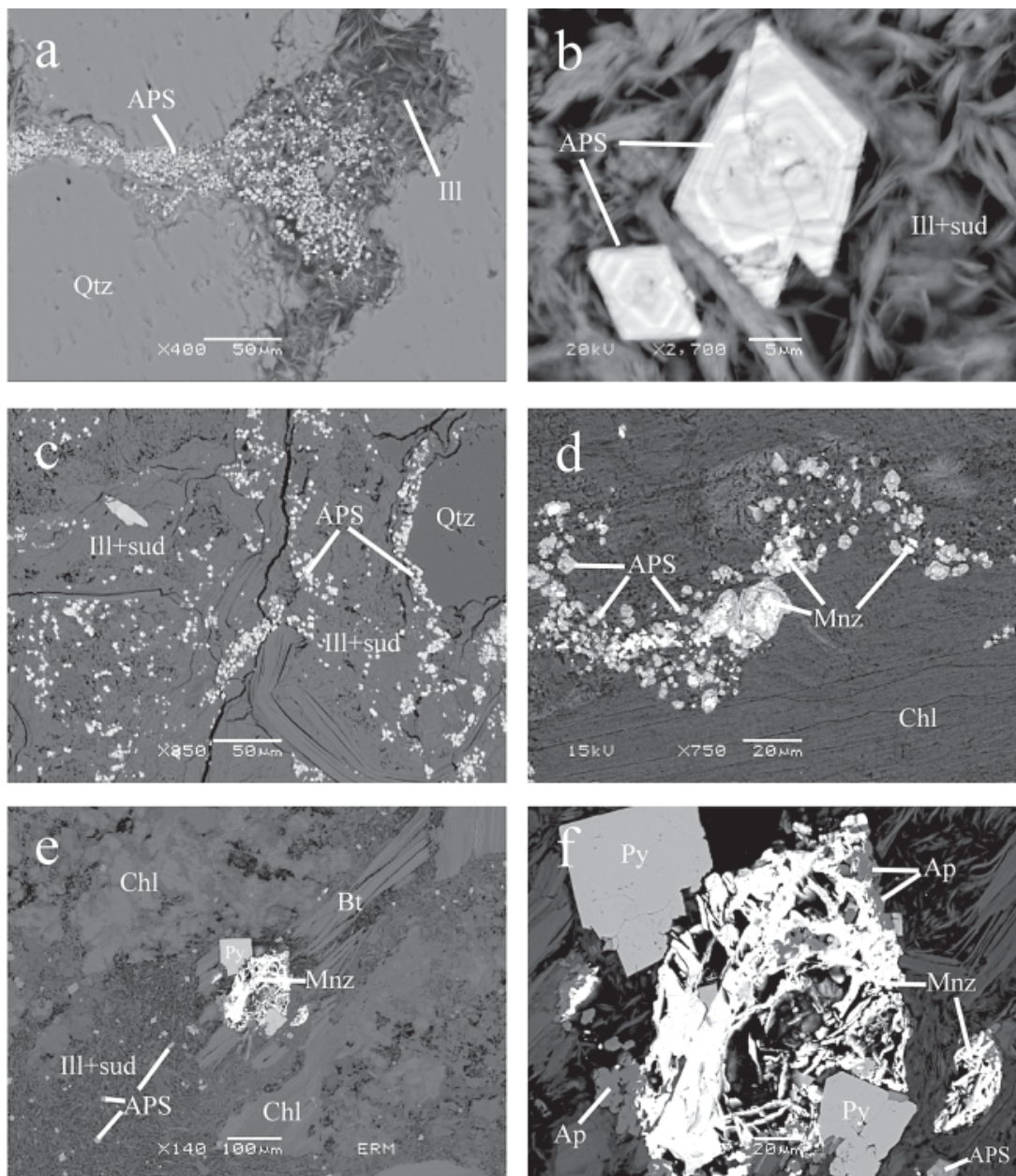
Fig. 2. SEM images of APS minerals from EARUF. a) Aggregate of small euhedral grains of APS minerals located in the intergranular pore-space of the clay matrix in a distal alteration area. b) Features of growth zoning of APS crystal in the basement rocks. c) Disseminated euhedral crystals of LREE–Sr Al-phosphates (white spots) in a matrix of hydrothermal illite–sudoite close to the major discontinuities. d) Monazite replaced by APS minerals in a sample of metamorphic basement almost totally chloritized (trioctahedral chlorite) close to the Ranger 3 uranium orebody of. e) Monazite relics in a clay matrix containing illite–clinochlore below the unconformity in an intermediate area of alteration. f) Alteration sites of monazite and pyrite, near which occur secondary apatite and APS associated with trioctahedral chlorite + illite below the unconformity in area of intermediate alteration. Symbols: APS aluminum phosphate–sulfate minerals, Ap apatite, Sud sudoite, Bt biotite, Chl trioctahedral chlorite, Ill illite, Mnz monazite, Py pyrite, and Qtz quartz.

the residue of altered monazite. These observations suggest that the dissolution of primary apatite was complete in the altered sandstones but only partial in the basement rocks. No direct replacement-induced feature of apatite involving the APS has been observed.

CHEMICAL RESULTS

Representative results of electron-microprobe analyses of APS minerals from the three zones of alteration distinguished in the above section are presented in Table 2. The chemical elements sought in individual crystals have been selected on the basis of preliminary qualitative EDS investigations. The low analytical total (between 60 and 85 wt%) obtained in some of the analyses is essentially due to the size of some APS grains (commonly <2 μm), which was commonly smaller than the volume of sample emitting the secondary X-ray radiation. Consequently, there is a partial integration of the surrounding minerals and micropores in the volume analyzed by the electron beam. It should be noted that the chemically variable zones observed in some APS crystals (Fig. 2b) are too thin to be analyzed individually with an electron microprobe.

All the analytical results agree with the general formula of APS minerals [$AB_3(XO_4)_2(OH)_6$]. They indicate a complex chemical composition corresponding to intimate mixtures or solid solutions among various compositional end-members, which combine essentially the following cations: Sr, LREE, Ca and Th at the A site, Al and Fe at the B site; P and S at the X site. Globally, the analytical results of APS crystals display a rather slight compositional variation in each given type of alteration zones, and a wide range of compositional variation from one type of alteration zone to another (Table 2). The major chemical variations measured in the APS from the different domains of alteration in the EARUF involve P, S, Sr and LREE (for comparison of these effects, the results of the analyses were normalized to 85 wt%, the anhydrous total in well-crystallized APS). The highest amounts of SrO and SO_3 (13.33 and 7.82 wt%, respectively) and the lowest amounts of $LREE_2O_3$ and P_2O_5 (6.33 and 22.49 wt%, respectively) were found in APS minerals from the distal zones of alteration, whereas the lowest amount of SrO and SO_3 (2.32 and 0.53 wt%, respectively), and the highest amounts of $LREE_2O_3$ and P_2O_5 (23.54 and 26.33 wt%, respectively) were found in APS minerals close to or from the Jabiluka, Ranger or Nabarlek orebodies. According to these results, Ce is the predominant LREE element encountered in the APS minerals close to the Jabiluka and Nabarlek deposits, whereas La predominates in the APS minerals close to the Ranger deposit. APS minerals from the intermediate alteration zones show amounts of P_2O_5, SO_3, SrO and $LREE_2O_3$ (24.07, 1.96, 4.24 and 17.43 wt%, respectively) intermediate but distinct from that of the other zones of alteration. The APS minerals from all the alteration zones identified in the EARUF contain minor but significant amounts of Ca and Th at their A site. Ca is roughly constant (CaO ranges from 1 to 2.3 wt%), whereas Th seems more variable, with lower amounts in APS from the zones of distal alteration and a slight enrichment in the APS surrounding the uranium deposits (ThO_2 ranges from 0.12 to more than 2 wt%). Aluminum is by far the dominant cation, in association with minor but variable amounts of Fe, in the B site of all the APS minerals. It should be noted that the uranium content of all the APS minerals analyzed is below the detection limit of the electron microprobe.

INTERPRETATION

Both the alteration petrography and the chemical data obtained in this study are used to discuss the significance of APS minerals in the alteration processes associated with uranium deposition in the EARUF. We will discuss these APS minerals successively in terms of crystal chemistry, element sources and signature of thermodynamic conditions of the alteration processes, which operated at a regional scale in the EARUF.

Crystal chemistry of APS minerals

The APS minerals from the EARUF have complex compositions that are seldom close to the pure end-members in the alunite supergroup described in the literature (Scott 1987, Dill 2001, Jambor 1999). Dill (2001) indicated that such a chemical feature is typical of APS from natural environments, which generally belong to several complex solid-solution series. The wide range of chemical compositions recorded in the APS throughout the altered zones at EARUF (Fig. 3) is essentially due to coupled substitutions of Sr for LREE and of S for P at the A and X sites, respectively. These substitutions change the relative proportion of end members of the beudantite group, namely svanbergite ($SrAl_3(PO_4, SO_4)(OH)_6$, and woodhouseite, $CaAl_3(PO_4, SO_4)(OH)_6$, and of the crandallite group, namely goyazite, $SrAl_3[PO_3 \bullet (O_{0.5}(OH)_{0.5})]_2(OH)_6$, crandallite, $CaAl_3[PO_3 \bullet (O_{0.5}(OH)_{0.5})]_2(OH)_6$, and florencite, $LREEAl_3(PO_4)_2(OH)_6$.

At every scale of observation, the major variation of the APS series essentially involves the relative proportion of svanbergite and florencite end-members. APS from the zones of distal alteration have a very distinctive compositional field, which differs from those of the intermediate and proximal zones of alteration by the predominance of svanbergite. Florencite predominates in the APS from both the intermediate and proximal zones of alteration, which form a compositional continuum. The proportion of florencite significantly increases in the APS series from intermediate to proximal zones of alteration.

Cross-plot diagrams between the major elements at the A and X sites of the APS (Fig. 4) indicate that the chemical variations are not exclusively due to a

svanbergite-to-florencite transition. The linear regression curves between all the data points do not conform to the ideal LREE-for-Sr and P-for-S substitutions involved in a svanbergite-to-florencite transition. A slight excess of Sr (5 to 10%) at very low S contents and a depletion of S (40 to 50%) at high Sr content should be noted. The cross-plot data for both S *versus* Sr and P *versus* Sr suggest that goyazite is associated with svanbergite and florencite in proportions that tend to decrease with decreasing distance from the orebodies. The Ca content of the APS does not significantly vary throughout the alteration areas at EARUF and seems to be mostly attributed to the crandallite end-member.

On the basis of the aforementioned chemical data, the mean composition of APS from each alteration area can be characterized as follows: 1) in the zones of distal alteration, $(Sr_{0.61}Ca_{0.21}LREE_{0.17}Th_{0.01})(Al_{2.89}Fe^{3+}_{0.11})[PO_3 \bullet (O_{0.76}(OH)_{0.24})]_{1.57}(SO_4)_{0.43}(OH)_6$, corresponding to a solid solution svanbergite$_{0.43}$ goyazite$_{0.18}$ crandallite$_{0.21}$ ThAl phosphates$_{0.01}$ florencite$_{0.17}$; 2) in the zones of intermediate alteration, $(Sr_{0.22}Ca_{0.16}LREE_{0.61}Th_{0.01})(Al_{2.93}Fe^{3+}_{0.07})[PO_3 \bullet (O_{0.88}(OH)_{0.12})]_{1.86}(SO_4)_{0.14}(OH)_6$, corresponding to a solid solution svanbergite$_{0.14}$ goyazite$_{0.08}$ crandallite$_{0.16}$ ThAl phosphates$_{0.01}$ florencite$_{0.61}$; 3) in the zones of proximal alteration, $(Sr_{0.09}Ca_{0.13}LREE_{0.76}Th_{0.02})(Al_{2.92}Fe^{3+}_{0.08})[PO_3 \bullet (O_{0.92}(OH)_{0.08})]_{1.96}[(SO_4)_{0.04}](OH)_6$, corresponding to a solid solution svanbergite$_{0.04}$ goyazite$_{0.05}$ crandallite$_{0.13}$ ThAl phosphates$_{0.02}$ florencite$_{0.76}$.

The overall variation of APS compositions determined above indicate an overall depletion in sulfates in the aqueous solutions, and conversely, a general enrich-

TABLE 2. RESULTS OF ELECTRON-MICROPROBE ANALYSES AND STRUCTURAL FORMULAS OF REPRESENTATIVE APS MINERALS ASSOCIATED WITH UNCONFORMITY-TYPE URANIUM DEPOSITS IN THE EAST ALLIGATOR RIVER URANIUM FIELD, AUSTRALIA

Sample				Proximal alteration areas				Intermediate alteration areas					Distal alteration areas	
		1			2			5			6			9	
		Mean*	σ		Mean	σ		Mean	σ		Mean	σ		Mean	σ
SrO wt%	2.24	1.68		2.06	1.66		4.03	4.32		3.90	3.13		12.02	12.28	
CaO	1.33	1.28		1.57	1.12		1.80	1.71		2.10	2.07		2.06	2.27	
La_2O_3	5.3	6.25		10.02	10.36		6.33	6.78		4.09	5.07		0.73	1.36	
Ce_2O_3	11.98	12.04		8.19	8.29		9.86	10.10		8.47	9.06		1.74	3.11	
Pr_2O_3	1.44	1.17		0.98	0.84		0.79	0.85		0.69	0.77		0.11	0.36	
Nd_2O_3	4.04	3.48		1.06	1.29		2.34	1.88		2.78	2.29		0.56	0.91	
ThO_2	0.77	0.75		1.61	0.83		0.43	0.42		0.98	1.21		0.27	0.48	
Al_2O_3	28.17	28.40		27.01	26.52		29.78	31.22		29.39	27.21		28.62	29.97	
Fe_2O_3	0.94	1.27		2.45	3.03		0.72	1.20		1.80	1.81		4.06	1.82	
P_2O_5	25.46	23.33		19.45	17.81		22.15	22.43		22.13	20.36		16.45	21.43	
SO_3	0.51	0.48		0.89	0.79		1.52	1.84		1.80	1.11		6.62	6.52	
Total	82.18	80.15		75.29	71.55		79.75	82.75		78.13	74.09		73.24	80.54	
A Sr *apfu*	0.12	0.09	0.02	0.11	0.10	0.01	0.20	0.22	0.02	0.21	0.17	0.03	0.67	0.61	0.05
Ca	0.13	0.13	0.05	0.16	0.13	0.02	0.17	0.16	0.01	0.21	0.21	0.02	0.21	0.21	0.02
La	0.17	0.21	0.03	0.35	0.39	0.04	0.20	0.22	0.01	0.14	0.17	0.03	0.03	0.04	0.01
Ce	0.39	0.40	0.05	0.28	0.29	0.01	0.32	0.32	0.01	0.29	0.31	0.02	0.06	0.09	0.02
Pr	0.05	0.04	0.01	0.03	0.03	0.01	0.03	0.03	0.00	0.02	0.03	0.00	0.00	0.01	-
Nd	0.13	0.11	0.02	0.04	0.05	0.01	0.07	0.06	0.01	0.09	0.08	0.01	0.02	0.03	0.01
Th	0.02	0.02	0.01	0.03	0.02	0.01	0.01	0.01	0.00	0.02	0.03	0.01	0.01	0.01	-
B Al	2.94	2.92	0.05	2.84	2.80	0.04	2.95	2.93	0.03	2.89	2.88	0.04	2.75	2.89	0.06
Fe	0.06	0.08	0.05	0.16	0.20	0.04	0.05	0.07	0.03	0.11	0.12	0.04	0.25	0.11	0.06
X P	1.96	1.96	0.01	1.92	1.92	0.02	1.89	1.86	0.02	1.87	1.91	0.02	1.47	1.57	0.06
S	0.04	0.04	0.01	0.08	0.08	0.02	0.11	0.14	0.02	0.13	0.09	0.02	0.53	0.43	0.06

Note: U_2O_3 is below the detection limit. * The mean was calculated on the basis of results of ten electron-microprobe analyses per sample. The structural formulae were calculated on the basis of one *A*-site cation, 2 (SO_4, PO_4) groups, and three (Al, Fe) *apfu* (atoms per formula unit).

ment in phosphate with increasing proximity to the uranium deposits. The concomitant enrichments of the APS in P and LREE toward the ore deposits suggests a common source and an extensive mobility of both sets of elements in the altered zones at EARUF.

Source material for APS minerals at EARUF

According to the wide range of environments documented for APS formation near the Earth's surface, the source materials for these minerals can be numerous. We have considered as source material the products of alteration (weathering, hydrothermal or diagenetic alteration) of primary minerals, including phosphates and REE-bearing minerals (Dill 2001), and the precipitation of reactive P and REE released from inorganic compounds during early diagenesis of clastic sediments (Rasmussen 1996). The source of the major elements incorporated in the APS minerals associated with the unconformity-type uranium deposits has never been investigated specifically. Several sources of elements have been proposed for the APS minerals formed in the Athabasca Basin, Canada. Diagenetic and hydrothermal alteration of detrital or early diagenetic clay and phosphate minerals of the siliciclastic formations during the basin evolution and the intense alteration of the metamorphic or magmatic monazite in the basement rocks are considered as the two best candidates for the release of the major elements incorporated in the APS on both sides of the unconformity (Wilson 1984, Fayek & Kyser 1997, Quirt *et al.* 1991, Hecht & Cuney 2000).

Monazite replacement by APS seems common, whereas no example of apatite replacement by APS has been observed. The parental links between monazite and APS, pointed out in our petrographic descriptions, are
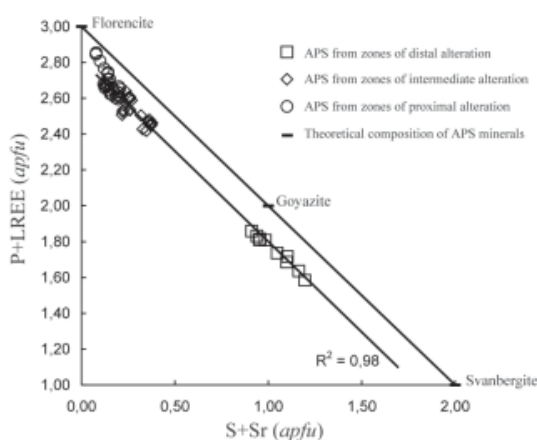

FIG. 3. Cross-plot diagram of P + LREE *versus* S + Sr showing the wide range of chemical compositions recorded in APS.

supported by geochemical considerations pertaining to the light rare-earths (LREE) and Th. Indeed, the relative proportions of cerium, lanthanum and neodymium measured in the APS minerals are close to those measured in the monazite residue (Fig. 5), which persists in the same altered samples of basement rocks or to a much lesser degree in sandstones (exclusively as inclusions in detrital quartz). In the same way, the increasing amount of LREE in APS minerals from distal to proximal areas of alteration is correlated with a slight increase of the average amount of Th, both suggesting a monazite source. No correlative enrichment in Ca accompanies the enrichment in P in the APS noted from distal to proximal zones of alteration, suggesting that apatite is not a major source of P and Ca.

All the above arguments indicate that the alteration of monazite represents the major source for the chemical elements (P, LREE and Th) involved in the compositional variations of APS between the distal and the proximal areas of alteration in the EARUF suite. Such an inference is an important clue to understand the geochemical links existing between the LREE-rich APS and the uranium deposits near where they are currently encountered. The monazite contains significant amounts of uranium, which was not incorporated in the products of alteration observed. Their U content is below the detection limit of the electron microprobe in the APS, whereas uranium-bearing minerals have been detected near the alteration sites of monazite only close to the uranium orebodies. At least a part of the uranium contained in the orebodies and most of the P, LREE and Th incorporated in APS minerals thus are genetically related. They are issued from the same process of alteration of monazite.

The source material of the svanbergite-rich APS, which characterizes the distal zones of alteration, is not clearly identified. However, the Sr-enriched APS probably originated during the burial diagenesis of the Kombolgie sandstones and could represent a stable phase in coexistence with the sub-basinal solutions of the diagenetic aquifers. Indeed, APS minerals with high Sr and S contents have frequently been reported in literature on sandstones worldwide (Rasmussen 1996, Spötl 1990, Dill 2001).

All the above considerations indicate that the crystal-chemical nature of APS in the Kombolgie sandstones could be indicative of the extent of alteration of monazite. The chemical trend of the APS (Fig. 6) leads us to interpret this as a signature of the degree of interaction between the diagenetic fluids from the Kombolgie sandstones (producing APS near the svanbergite end-member) with solutions enriched in P, LREE and Th (close to the florencite end-member). In agreement with the genetic model and the alteration patterns proposed for the EARUF unconformity-type uranium deposits (Komninou & Sverjensky 1996, Beaufort *et al.* 2005), this origin could relate to the alteration of monazite within the underlying basement rocks.

APS minerals: markers of thermodynamic conditions

The chemical trend exhibited by the APS from the EARUF suggests that their compositional variation is controlled by large-scale variations in their physicochemical conditions of formation. Thermodynamic calculations have been made to shed light on the respective stability of svanbergite, goyazite, and florencite end-members.

The thermodynamic calculations have been performed for the following conditions: 1) constant temperature and pressure fixed at 200°C and 500 bars, in agreement with the data already used for geochemical modeling (Komninou & Sverjensky 1996, Iida 1993) or

obtained from fluid-inclusion studies (Derome *et al.* 2003) of the EARUF unconformity-type uranium deposits; 2) tetravalent cerium has been neglected because this ion is stable only in extremely oxidizing conditions; 3) a constant content of aluminum was assumed in all the APS relations, and 4) the effect of pressure on equilibrium between any two phases has been neglected.

Gibbs free energies of formation of these APS end members are given in Table 3. Entropy and heat capacities of APS minerals were estimated from experimental values for alunite and jarosite by the method proposed by Helgeson *et al.* (1978). Enthalpies of formation were calculated from Gibbs free energies of formation and entropy given in Table 3. Equilibrium constants for the
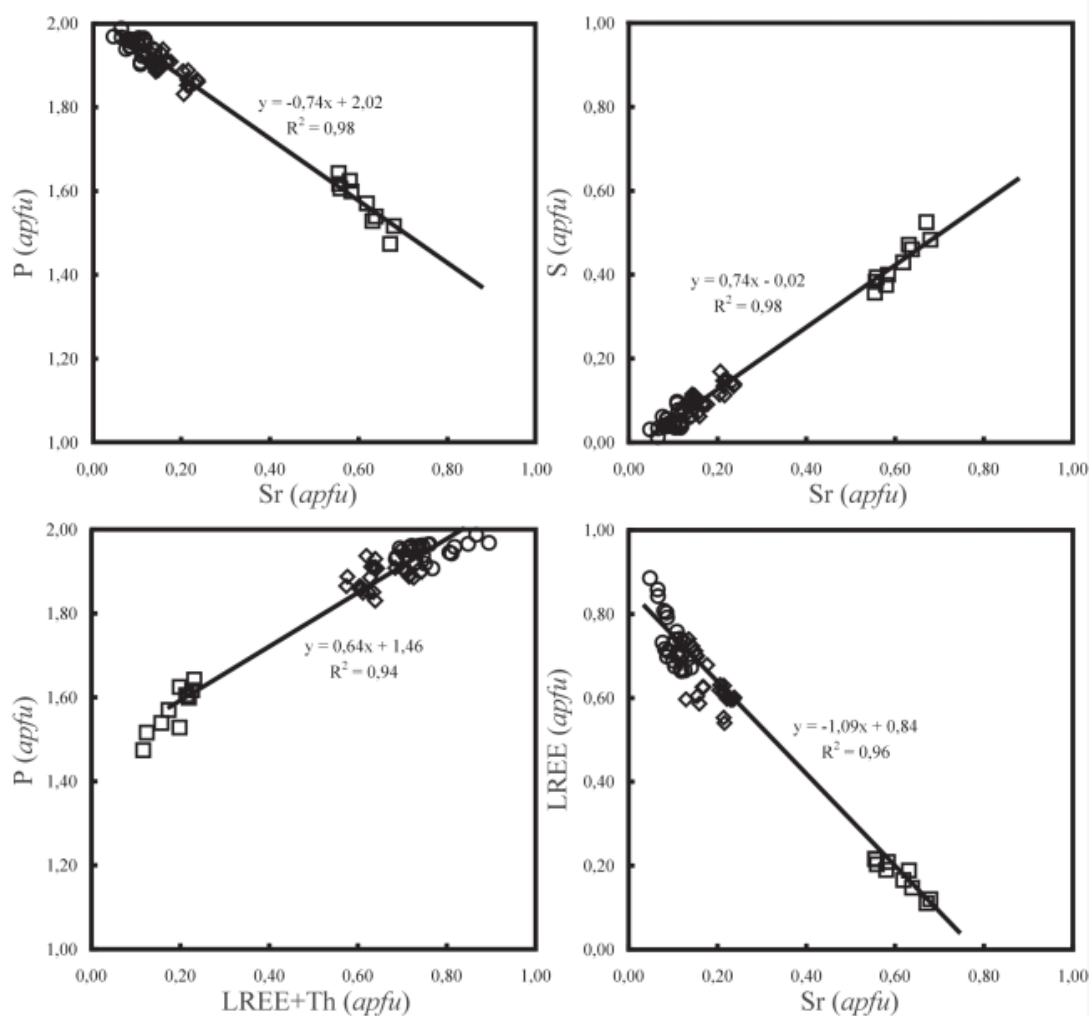

FIG. 4.   Cross-plot diagrams showing the major elements at the *A* and *X* sites in the different APS minerals encountered in all the different geological units surrounding the EARUF deposits or prospects. □ APS from zones of distal alteration, ◇ APS from zones of intermediate alteration, and ○ APS from zones of proximal alteration.
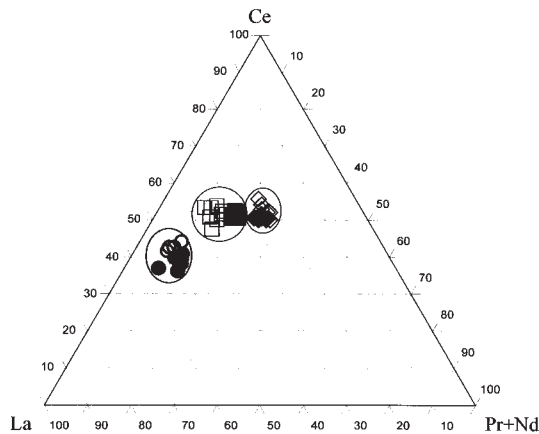
FIG. 5. Projection in terms of Ce – La – (Nd + Pr) (elecron-microprobe data) of the various monazite and APS minerals for a given sample encountered in all the geological units surrounding the EARUF deposits or prospects. Sample 2, proximal alteration: ● monazite, ○ APS minerals. Sample 5, intermediate alteration: ◆ monazite, ◇ APS minerals. Sample 7, intermediate alteration: ■ monazite, □ APS minerals.

dissolution reactions of the APS minerals were calculated with the SUPCRT program (Johnson *et al.* 1992) and are given in Table 4.

The stability domains of svanbergite, goyazite, and florencite have been plotted in a log $[Sr^{2+}/Ce^{3+}]$ *versus* pH for two different values of $f(O_2)$ and for total phosphorus (P_T) and total sulfur (S_T) maintained constant. It can be seen that the stability of these minerals is highly sensitive to pH. Svanbergite is the stable APS end-member at low pH and relatively oxidizing conditions, *i.e.*, at $f(O_2)$ equal 10^{-30} atm (Fig. 7a). More reducing conditions in the system, *i.e.*, at $f(O_2)$ equal to 10^{-38} atm (Fig. 7b), will strongly narrow the stability domain of svanbergite toward still more acidic conditions and hence promote the stability of goyazite at high Sr^{2+}:Ce^{3+} ratio, or florencite at lower Sr^{2+}:Ce^{3+} ratio. In other words, the transition svanbergite to florencite exhibited by APS minerals around the EARUF unconformity-type deposits can be explained by concomitant increase of pH and reducing conditions and decrease of the Sr^{2+}:Ce^{3+} ratio in the hydrothermal solutions. No data exist on the Sr^{2+}:Ce^{3+} ratio of the fluids associated with the uranium deposition in the EARUF unconformity-type deposits. However, on the basis of petrography, it seems reasonable to consider that the Sr^{2+}:Ce^{3+} ratio is strongly dependent on the degree of interaction between the acidic diagenetic solutions and monazite in the basement rocks.
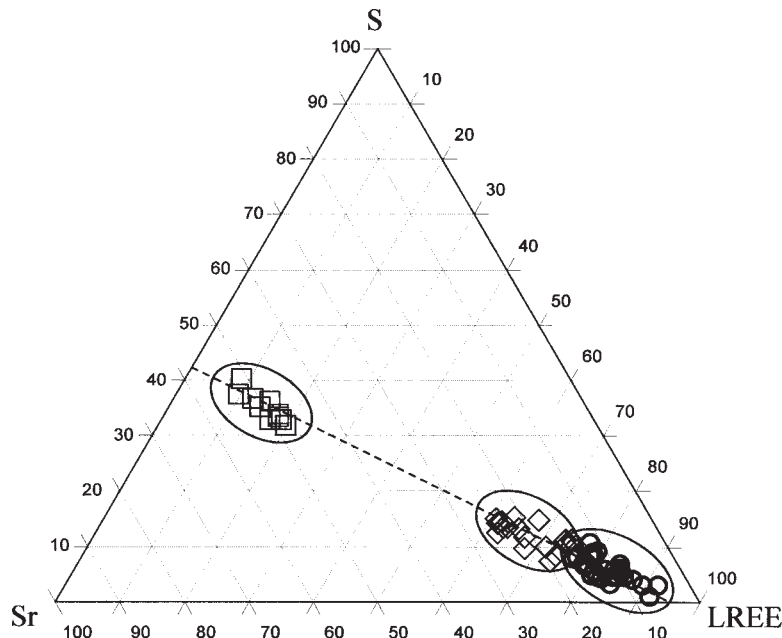

FIG. 6. Projection in terms of S – Sr – LREE (electron-microprobe data) for the various APS minerals encountered in all the geological units surrounding the EARUF deposits or prospects. ○ APS minerals from zones of proximal alteration, ◇ APS minerals from zones of intermediate alteration, □ APS minerals from zones of distal alteration.

Concluding Remarks

The results of this study indicate that the APS minerals are genetically related to the alteration features associated with uranium deposition in the unconformity-type deposits of the East Alligator River Uranium Field. The APS minerals are mostly products of alteration of monazite and present significant compositional variations. These depend on chemical factors that are consistent with those proposed in the genetic models for unconformity-type uranium deposits. These models involve the interaction of hypersaline, oxidizing and relatively acidic fluids (*i.e.*, sub-basinal brines derived from

the overlying sandstones) with the underlying basement-rocks (Plant *et al.* 1999) and development of redox and pH fronts during the overall process of alteration (Hoeve & Quirt 1984). Once these fluids moved into the basement, they were progressively reduced by interaction with reducing agents such as graphite or ferrous-iron-bearing minerals, and the pH of the fluid was increased during the alteration. A major proportion of the uranium in these deposits was deposited in zones of the basement where high degrees of reduction and neutralization of the hydrothermal fluids were attained.

We suggest here that the transition from svanbergite to florencite in the APS series is a good marker to in-

TABLE 3. THERMODYNAMIC VALUES FOR SOME MINERALS
OF THE ALUNITE SUPERGROUP AT 25°C

Mineral	ΔG°_f kJ• mol^{-1}	ΔH°_f kJ• mol^{-1}	S° J•K^{-1}• mol^{-1}	V cm^3• mol^{-1}	a J•K^{-1}• mol^{-1}	$b \times 10^3$ J•K^{-2}• mol^{-1}	$c \times 10^{-5}$ J•K• mol^{-1}
Florencite	-5737.52[1]	-6256.17[3]	330.28[4]	137.517	366.39[6]	352.84[6]	-64.89[6]
Goyazite	-5625.39[1]	-6159.27[3]	321.87[4]	142.126	363.33[5]	369.03[5]	-60.15[5]
Svanbergite	-5286.61[2]	-5752.50[3]	508.84[4]	142.270	408.69[6]	264.32[6]	-73.62[6]

(1) Schwab *et al.* (1993); (2) Gaboreau & Vieillard (2004); (3) calculated from S°; (4) estimate from S° of alunite by the algorithm method of Helgeson *et al.* (1978); (5) Stoffregen *et al.* (2000); (6) estimate from Cp of alunite by the algorithm of Helgeson *et al.* (1978).
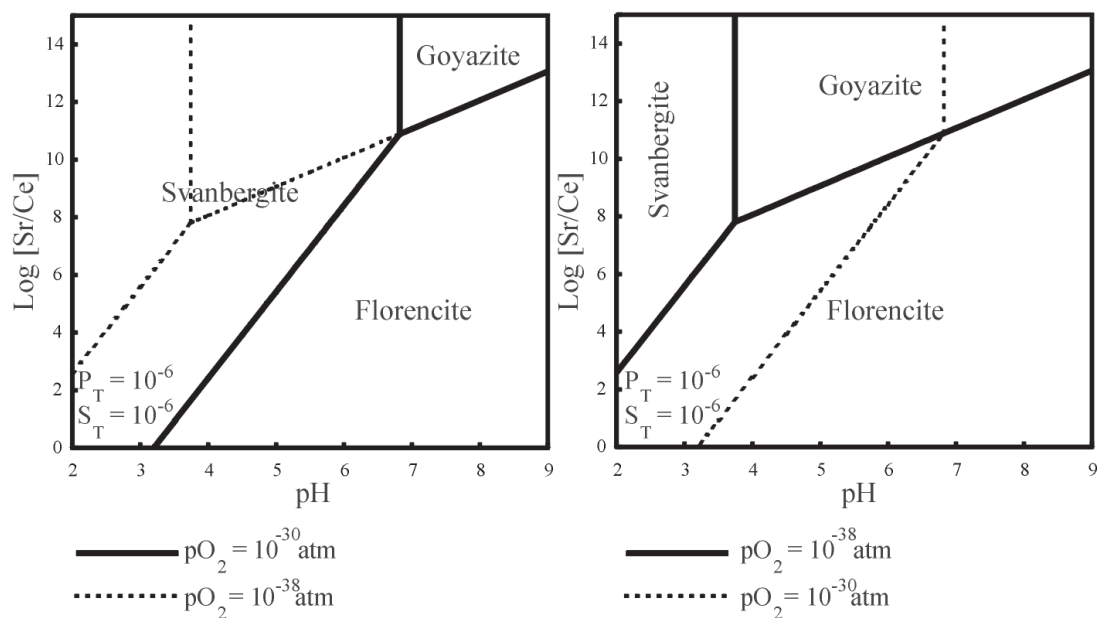

Fig. 7.   Activity–activity diagrams log [Sr^{2+}/Ce^{3+}] *versus* pH representing the stability domains of svanbergite, goyazite, florencite for two different values of log $a(O_2)$.

TABLE 4. SOLUBILITY PRODUCTS OF DISSOLUTION REACTIONS OF THE APS MINERALS
AT 25°, 200°C AND 500 BARS

Mineral	Dissolution reaction	Log K 25°C	Log K 200°C
Florencite	$CeAl_3(PO_4)_2(OH)_6 + 12H^+ \Rightarrow Ce^{3+} + 3Al^{3+} + 2H_3PO_4 + 6H_2O$	19.544	–5.491
Goyazite	$SrAl_3[PO_3\bullet O_{0.5}(OH)_{0.5}]_2(OH)_6 + 11H^+ \Rightarrow Sr^{2+} + 3Al^{3+} + 2H_3PO_4 + 6H_2O$	19.628	–1.429
Svanbergite	$SrAl_3(PO_4,SO_4)(OH)_6 + 9H^+ \Rightarrow Sr^{2+} + 3Al^{3+} + H_3PO_4 + SO_4^{2-} + 6H_2O$	9.991	–11.257

vestigate the distribution of the pH front that results from the interaction of the diagenetic solutions with the basement rocks below the unconformity. Svanbergite-rich APS minerals were formed only from diagenetic reactions in the Kombolgie sandstones, whereas the florencite content of APS increases with increasing degree of alteration of monazite-bearing rocks (mostly basement rocks). The transition from florencite-rich APS to apatite, which was observed at various scales (*i.e.*, alteration assemblages near individual grains of monazite or regional zoning in basement rocks), is also consistent with a higher degree of neutralization of acidic diagenetic fluids by interaction with basement rocks. Indeed, APS minerals are known to be more stable in lower-pH environments (in which LREE are relatively mobile) than apatite (Spötl 1990, Stoffregen & Alpers1987, Vieillard *et al.* 1979).

Further investigations are needed to determine the extent of the various solid-solutions in APS minerals from unconformity-type uranium deposits, before one can proceed to use them as an appropriate indicator of paleoconditions and hence as a potential tool in mineral exploration. We would like to see a comparative study of the composition of APS minerals from the Proterozoic basins in Canada, containing high-grade uranium orebodies (Athabasca, Thelon), the use of thermodynamic models integrating solid-solutions for both the APS and the associated clay minerals, and isotope studies on purified mineral fractions (stable and unstable). These additional investigations are required to test the general validity of our present findings and will contribute to improve our knowledge concerning the conditions of formation (P, Eh, pH) of such uranium deposits.

ACKNOWLEDGEMENTS

REFERENCES

BEAUFORT, D., PATRIER, P., LAVERRET, E., BRUNETON, P. & MONDY, J. (2005): Clay alteration associated with Proterozoic unconformity-type uranium deposits in the East Alligator River uranium field (Northern Territory, Australia). *Econ. Geol.* (in press).

DEROME, D., CUNEY, M., CATHELINEAU, M., FABRE, C., DUBESSY, J., BRUNETON, P. & HUBERT, A. (2003): A detailed fluid inclusion study in silicified breccias from the Kombolgie sandstones (Northern Territory, Australia): application to the genesis of middle Proterozoic unconformity-type uranium deposits. *J. Geochem. Explor.* **80**, 259-275.

DILL, H.G. (2001): The geology of aluminium phosphates and sulphates of the alunite group minerals: a review. *Earth-Sci. Rev.* **53**, 35-93.

FAYEK, M. & KYSER, T.K. (1997): Characterization of multiple fluid-flow events and rare-earth-element mobility associated with formation of unconformity-type uranium deposits in the Athabasca Basin, Saskatchewan. *Can. Mineral.* **35**, 627-658.

GABOREAU, S. & VIEILLARD, P. (2004): Prediction of Gibbs free energies of formation of minerals of the alunite supergroup. *Geochim. Cosmochim. Acta* **68**, 3307-3316.

GUSTAFSON, L.B. & CURTIS, L.W. (1983): Post Kombolgie metasomatism at Jabiluka, Northern Territory, Australia, and its significance in the formation of high grade uranium mineralization in lower Proterozoic rocks. *Econ. Geol.* **78**, 26-56.

HECHT, L. & CUNEY, M. (2000): Hydrothermal alteration of monazite in the Precambrian crystalline basement of the Athabasca basin (Saskatchewan, Canada): implications for the formation of unconformity-related uranium deposits. *Mineral. Deposita* **35**, 791-795.

HELGESON, H.C., DELANY, J.M., NESBITT, H.W. & BIRD, D.K. (1978): Summary and critique of the thermodynamic properties of the rock-forming minerals. *Am. J. Sci.* **278–A**, 1-229.

HOEVE, J. & QUIRT, D. (1984): Mineralization and host rock alteration in relation to clay mineral diagenesis and evolution of the middle-Proterozoic Athabasca Basin, northern Saskatchewan, Canada. *Saskatchewan Research Council, Tech. Rep.* **187**.

IIDA, Y. (1993): Alteration and ore forming processes of unconformity related uranium deposits. *Resource Geol.* **15**, 299-308.

JAMBOR, J.L. (1999): Nomenclature of the alunite supergroup. *Can. Mineral.* **37**, 1323-1341.

JOHNSON, J.W., OELKERS, E.H. & HELGESON, H.C. (1992): SUPCRT 92: a software package for calculating the standard molal thermodynamic properties of minerals, gases, aqueous species and reactions from 1 to 5000 bars and 0°C to 1000°C. *Comput. Geosci.* **18**, 899-947.

KOLITSCH, U. & PRING, A. (2001): Crystal chemistry of the crandallite, beudantite and alunite groups: a review and evaluation of the suitability as storage materials for toxic metals. *J. Mineral. Petrol. Sci.* **96**, 67-78.

KOMNINOU, A. & SVERJENSKY, D.A. (1996): Geochemical modeling of the formation of an unconformity-type uranium deposit. *Econ. Geol.* **91**, 590-606.

KYSER, K., HIATT, E., RENAC, C., DUROCHER, K., HOLK, G. & DECKART, K. (2000): Diagenetic fluids in paleo- and meso-Proterozoic sedimentary basins and their implications for long protracted fluid histories. *In* Fluids and Basin Evolution (T.K. Kyser, ed.). *Mineral. Assoc. Can., Short Course Vol.* **28**, 225-262.

LORILLEUX, G. (2001): Les brèches associées aux gisements d'uranium de type discordance du bassin d'Athabasca, Saskatchewan, Canada. Thèse doctorale, Univ. Nancy, Nancy, France.

MAAS, R. (1989): Nd–Sr isotope constraints on the age and origin of unconformity-type uranium deposits in the Alligator River uranium field, Northern Territory, Australia. *Econ. Geol.* **84**, 64-90.

MILLER, A.R. (1983): A progress report: uranium–phosphorus association in the Helikian Thelon Formation and sub-Thelon saprolite, central District of Keewatin. *Geol. Surv. Can., Pap.* **83–1A**, 449-456.

MORDBERG, L.E., STANLEY, C.J. & GERMANN, K. (2000): Rare earth element anomalies in crandallite group minerals from the Schugorsk bauxite deposit, Timan, Russia. *Eur. J. Mineral.* **12**, 1229-1243.

NEEDHAM, R.S. (1988): Geology of the Alligator River uranium field, Northern Territory. *Bur. Mineral Resources, Bull.* **96**.

NUTT, C.J. (1989): Chloritization and associated alteration at the Jabiluka unconformity-type uranium deposit, Northern Territory, Australia. *Can. Mineral.* **27**, 41-58.

OJAKANGAS, R.W. (1986): Sedimentology of the basal Kombolgie Formation, Northern Territory, Australia: a Proterozoic fluvial quartzose sequence. *In* Sediments Down Under. Int. S.-B.M.R. Australia. Highland Press, Fishwick, Canberra, Australia.

PATRIER, P., BEAUFORT, D. & BRUNETON, P. (2003): Dickite and 2M_1 illite in deeply buried sandstones from the middle Proterozoic Kombolgie Formation (Northern Territory, Australia). *Clays Clay Minerals* **51**, 102-116.

PLANT, J.A., SIMPSON, P.R., SMITH, B. & WINDLEY, B.F. (1999): Uranium ore deposits – products of the radioactive earth. *In* Uranium: Mineralogy, Geochemistry and the Environment (P.C. Burns & R. Finch, eds.). *Rev. Mineral.* **38**, 255-319.

QUIRT, D., KOTZER, T. & KYSER, T.K. (1991): Tourmaline, phosphate minerals, zircon and pitchblende in the Athabasca group: Maw Zone and McArthur River Areas, Saskatchewan. *Saskatchewan Geol. Surv., Tech. Rep.* **91-4**, 181-191.

RASMUSSEN, B. (1996): Early-diagenetic REE-phosphate minerals (florencite, gorceixite, crandallite, and xenotime) in marine sandstones: a major sink for oceanic phosphorus. *Am. J. Sci.* **296**, 601-632.

SCHWAB, R.G., GOTZ, C., HEROLD, H. & OLIVEIRA, N.P. (1993): Compounds of the crandallite type – thermodynamic properties of Ca-phosphates, Sr-phosphates, Ba-phosphates, Pb-phosphates, La-phosphates, Ce-phosphates to Gd-phosphates and Ca-arsenates, Sr-arsenates, Ba-arsenates, Pb-arsenates, La-arsenates, Ce-arsenate. *Neues Jahrb. Mineral., Monatsh.*, 551-568.

SCOTT, K.M. (1987): Solid solution in, and classification of, gossan-derived members of the alunite–jarosite family, northwest Queensland, Australia. *Am. Mineral.* **72**, 178-187.

SPÖTL, C. (1990): Authigenic aluminium phosphate–sulphates in sandstones of the Mitterberg Formation, northern Calcareous Alps, Austria. *Sedimentology* **37**, 837-845.

STOFFREGEN, R.E. (1993): Stability relations of jarosite and natrojarosite at 150–250°C. *Geochim. Cosmochim. Acta* **57**, 2417-2429.

_____ & ALPERS, C.N. (1987): Woodhouseite and svanbergite in hydrothermal ore deposits: products of apatite destruction during advanced argillic alteration. *Can. Mineral.* **25**, 201-211.

_____, _____ & JAMBOR, J.L. (2000): Alunite–jarosite crystallography, thermodynamics, and geochronology. *In* Sulfate Minerals – Crystallography, Geochemistry, and Environmental Significance (C.N. Alpers, J.L. Jambor & D.K. Nordstrom, eds.). *Rev. Mineral. Geochem.* **40**, 453-479.

_____, RYE, R.O. & WASSERMAN, M.D. (1994): Experimental studies of alunite. I. ^{18}O–^{16}O and D–H fractionation factors between alunite and water at 250–450°C. *Geochim. Cosmochim. Acta* **58**, 903-916.

SWEET, I.P., BRAKEL, A.T. & CARSON, L. (1999): The Kombolgie Subgroup, a new look at an old "formation". *AGSO Res. Lett.* **30**, 26-28.

VIEILLARD, P., TARDY, Y. & NAHON, D. (1979): Stability fields of clays and aluminum phosphates: parageneses in lateritic weathering of argillaceous phosphatic sediments. *Am. Mineral.* **64**, 626-634.

WILDE, A.R., MERNAGH, T.P., BLOOM, M.S. & HOFFMANN, C.F. (1989): Fluid inclusion evidence of the origin of some Australian unconformity-related uranium deposits. *Econ. Geol.* **84**, 1627-1642.

WILSON, J.A. (1984): Crandallite group minerals in the Helikian Athabasca group in Alberta, Canada. *Can. J. Earth Sci.* **22**, 637-641.